



**AAS 02-063  
(DRAFT - 1)**

## Energy Storage Flywheels on Spacecraft

Robert O. Bartlett<sup>\*</sup>, Gary Brown<sup>‡</sup> and Joel Levinthal<sup>\*</sup>

<sup>\*</sup> AFS Trinity Power Corp

<sup>‡</sup> NASA, Goddard Space Flight Center

---

### 25th ANNUAL AAS GUIDANCE AND CONTROL CONFERENCE

---

February 6-10, 2002  
Breckenridge, Colorado

Sponsored by  
Rocky Mountain Section



AAS Publications Office, P.O. Box 28130 - San Diego, California 92198

## **Abstract**

With advances in carbon composite material, magnetic bearings, microprocessors, and high-speed power switching devices, work has begun on a space qualifiable Energy Momentum Wheel (EMW). An EMW is a device that can be used on a satellite to store energy, like a chemical battery, and manage angular momentum, like a reaction wheel. These combined functions are achieved by the simultaneous and balanced operation of two or more energy storage flywheels. An energy storage flywheel typically consists of a carbon composite rotor driven by a brushless D.C. motor/generator. Each rotor has a relatively large angular moment of inertia and is suspended on magnetic bearings to minimize energy loss. The use of flywheel batteries on spacecraft will increase system efficiencies (mass and power), while reducing design-production time and life-cycle cost.

Mass savings not only rise from the flywheel battery's superior specific energy (including controller electronics and harness) and increased depth of discharge over traditional spacecraft batteries, but also from the elimination of separate reaction/momentum control hardware. The use of flywheel batteries will also lead to mass and cost savings in the satellite power system and thermal control by reducing power system losses. Lower losses will lead to reductions in the size and cost of the thermal control system and solar array. The flywheel battery will have a nominal thermal operating range typical of other spacecraft components (0°C to 40°C) and eliminate the need for a battery mounting cold-plate. Other cost savings and reliability improvements will occur through the elimination of test batteries, flight battery change-outs, and pre/post-launch recondition of batteries.

This paper will present a discussion of flywheel battery design considerations and a simulation of spacecraft system performance utilizing four flywheel batteries to combine energy storage and momentum management for a typical LEO satellite. A proposed set of control laws and an engineering animation will also be presented. Once flight qualified and demonstrated, space flywheel batteries may alter the architecture of most medium and high-powered spacecraft.

## **1. Introduction**

While the concept of an Energy Momentum Wheel (EMW) for spacecraft use has been studied for many year (Tsiotras, 1999, see references), it is only in the last ten years that enabling technologies such as microprocessors, high-strength composites, advanced magnetic bearings, and high-power solid state switches have evolved. The EMW offers to potential to increase satellite system efficiencies (mass and power), reduce design-production time, and reduce life-cycle cost of satellite systems. Active magnetic bearing technology, in particular, is of critical importance for an efficient and effective EMW. Spacecraft specifications often require stringent pointing requirements as well as a vibration-free environment for onboard experiments. Imbalances and natural frequency modes in the EMW can create inertia forces which, when interacting with the stator, will

transmit unwanted vibrations into the spacecraft structure. This can be avoided with the use of active magnetic bearings. The successful development of an effective magnetic bearing controller is a critical technology for the EMWs use in satellites. Advances in the control of EMW magnetic bearings have been reported recently (Zorzi, 2001, and Luo, 2000).

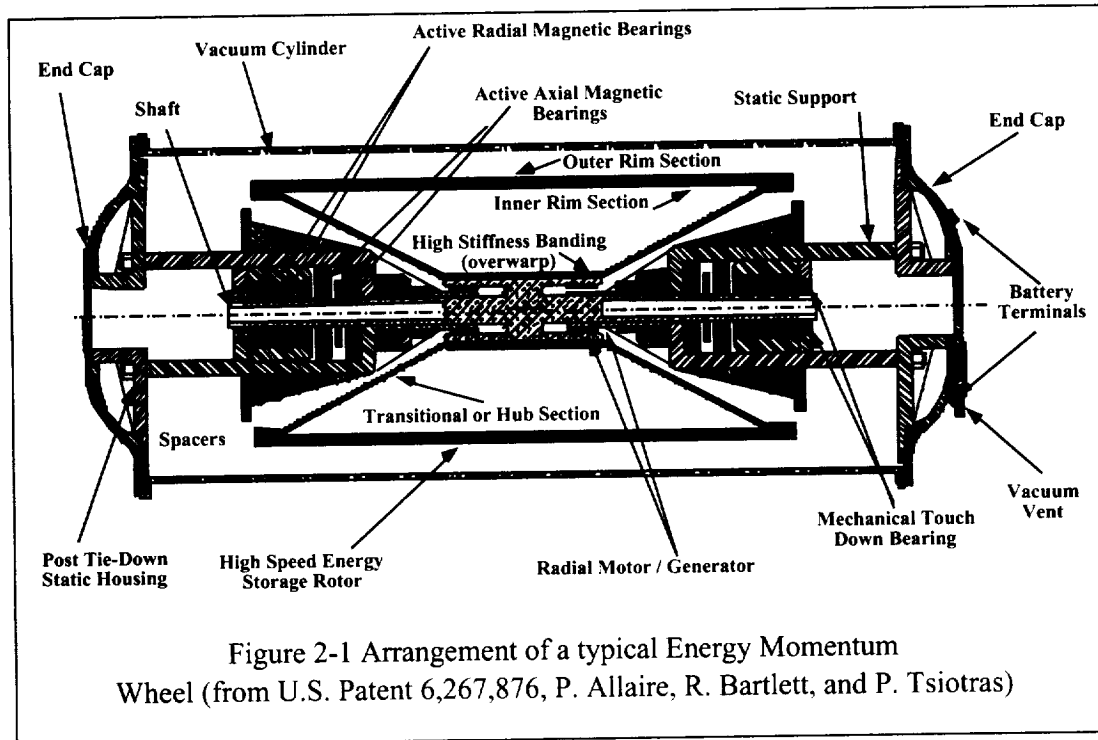
In the following sections a general introduction to the elements and configuration of a typical EMW will be presented and a few of the considerations for the application of this device to a spacecraft power and control system will be discussed. A high fidelity digital simulation of an EMW integrated into a spacecraft power and control system model has been developed and initial simulation results will be presented. NASA Glenn Research Center recently awarded a contract to Lockheed Martin CSS, Newtown, PA, to perform a laboratory demonstration of three EMWs and associated electronics as required to integrate energy storage and momentum management. This demonstration, called the COordinated Momentum and Energy Transfer (COMET) using EMWs, will validate Lockheed Martin's recently invented energy storage and attitude control concept (patent pending). AFS Trinity is providing the laboratory type EMWs to support this demonstration.

## **2. Description of Energy Momentum Wheel**

An Energy Momentum Wheel (EMW) is a deceptively simple device. While it is a concept that has been considered for spacecraft application for about twenty-five years, it remains a complex and highly integrated electro-mechanical system. Alter just one component and you will most likely have to modify another, if not all of the components. The interrelationships of designing for: managed magnetic forces, thermal effects, mechanical stresses, dissimilar materials, stable and robust control architecture, high-speed operation and corresponding frequencies, etc., is complex. The intricacy is even further exasperated by the nature of the association and the strongly non-linear interrelationships.

The elements on an EMW are illustrated per Figure 2-1. AFS Trinity's development and hardware test program has focused upon qualification of these specially designed and attuned components. An important step in quantifying the operational characteristics of the AFS Trinity system design is successful operation of the sub-system components. This hardware includes the high-speed composite rotor-bearing sub-system, coupled to a permanent magnet brushless dc motor/generator and operating to high-speeds in a vacuum. Attention to issues such as; safety, advanced controls, rotor-dynamics stability, component losses, structural design, material selection, in-situ balancing, are but a few of the considerations which have been included in the formulation of the AFS Trinity development and test program. The AFS Trinity program also integrates advanced rotor, magnetic bearings, motor/generator, controls and system technology as developed by AFS Trinity over the past seven years.

A major driver in AFS Trinity's design philosophy is minimal energy loss. Motor/generator and active magnetic suspension system losses reduce the availability of



stored energy for satellite power, and may also induce heat transfer difficulties, thermal operational limitations and life limiting consequences. If system losses are to be properly quantified then the motor/generator and magnetic suspension must be carefully evaluated at frequencies characteristic of operational environment. To reach those higher frequencies of operation the system must be carefully designed and evaluated prior to test. AFS Trinity recognizes that the successful operation of a complex rotor system at speeds reaching 80,000 rpm is challenging. It is often been asserted that problems associated with development and running such high-speed flywheel systems are due to one of the component's deficiency. More specifically it is often stated that the bearings are the culprit prohibiting high-speed successful operation. In truth decades of experience with modern high-speed equipment has taught its lessons very well. The problems associated with such system operation are most likely due to component interaction and/or integration and not generally the fault of isolated components. Therefore, AFS Trinity paid particular attentions to system integration issues, as well as safe reliable component design. It is anticipated that our development/test program will demonstrate a performance standard not previously unattained for low loss magnetic bearings.

The major EMW components include:

- 2.1 Rotor Shaft Assembly The AFS Trinity rotor shaft assembly consists of a rotor assembled with multiple, wet filament wound, filamentary composite rings, and mounted on the rotor shaft. The AFS Trinity baseline rotor, shown in Figure 2-1, offers 3.5k Whr of useable energy. This design approach enhances not only all major areas of performance including specific energy (Whr/kg) of the rotor, but it can have a dramatic positive effect on the rest of the EMW, especially the magnetic bearings. The rotor design is a derivative of the ORNL rotor (Figure 2-2) that was developed for AFS. The rotor design utilizes two nested rings of filament wound T-1000G composite integrated with a composite hub.



Figure 2-2 AFS Trinity High Specific Energy Rotor Assembly Parts Developed under contract at the Oak Ridge National Laboratory

Additional rotor designs will be developed in parallel to the ongoing test efforts. AFS Trinity implements NISA finite element software and AFS Trinity proprietary software for this effort. It is noteworthy that the current test system configuration permits AFS Trinity test capability to include advanced rotor designs, such as the higher specific energy flywheel components shown in Figure 2-1.

- 2.2 Motor/Generator AFS Trinity contracted the development of a 3 kW low loss motor/generator (Figure 2-3). This permanent magnet machine is a rugged and simple and is capable of very high-speed operation. By using the composite rotor to hold the rare earth magnets in position, speeds in excess of 60 KRPM have already been achieved and very high efficiencies were demonstrated. The motor/generator produces an effectively constant torque over the EMW operating range. These devices can utilize a number of sensor options to provide commutation control for the driver electronics. The absence of excitation winding on the rotor eliminates rotor copper losses, resulting in higher efficiency as compared to other machines.

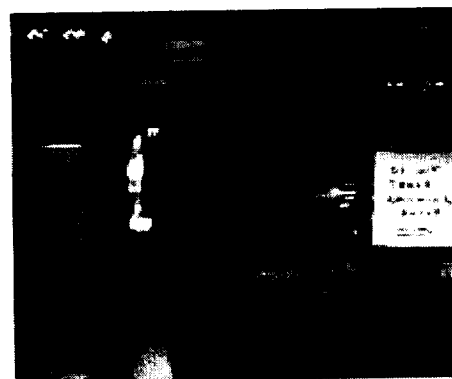


Figure 2-3 AFS Trinity Motor/Generator In-bench Test at Honeywell Space Satellite Systems

- 2.3 Magnetic Axial and Radial Bearings AFS Trinity's effort to improve the performance and efficiency of magnetic bearings has spanned several years. AFS Trinity has not

been satisfied with just approaching the challenge through modified mechanical hardware but instead has supported development of new and robust controllers. Previous control algorithms for magnetic bearing-supported flywheels do not have the desired adaptive control properties needed for the EMW. AFS Trinity plans to utilize control algorithms that will further reduce vibration and reduce losses, further improving efficiency. In addition, the AFS Trinity mechanical design pays special attention to important elements, such as minimal lamination thickness to reduce eddy current losses. AFS Trinity magnetic bearing research and development, sponsored in part by NASA, is proceeding at the University of Virginia (UVA), who produced the magnetic bearings shown in Figure 2-4.

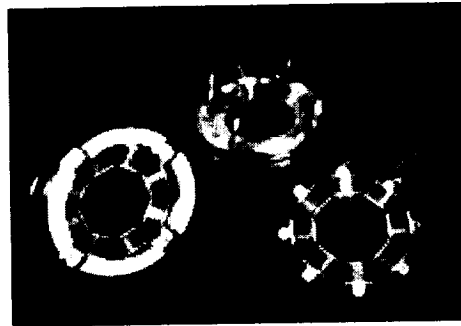
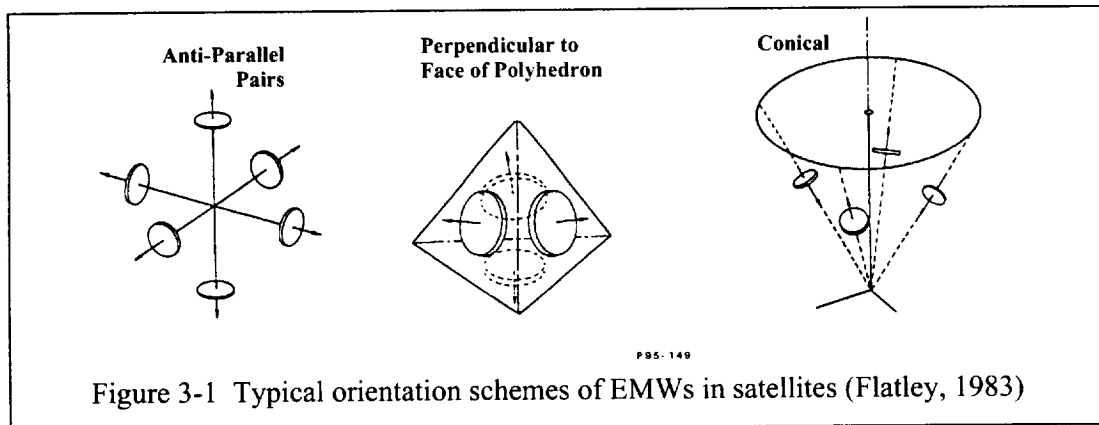


Figure 2-4 UVA Magnetic Bearings Operated at 100k RPM

- 2.4 **Touchdown Bearings** Touchdown bearings support the rotor system for rotating assembly coast-down in the event of an electrical failure and/or as catcher bearings in the event of unanticipated loads which may overload the magnetic suspension. Generally this component has received less than full attention to its important mission. In the event of a rotor drop onto the backup bearings the transient response of the rotor must be quickly dissipated to a safe operating state. These transient rotor loads, including simulations of gyroscopic loading, rotor stability etc. are routinely modeled by AFS Trinity personnel using proprietary rotor-dynamic software. The attention to additional damping resources such as elastomeric or eddy-current, to further aid the touchdown bearing in its mission, is now under consideration. It is also noteworthy that AFS Trinity has spent considerable efforts with pin-on-disk tribology testing of material and lubricant combinations to develop touchdown bearings capable of thousands of cycles, rapid acceleration and abusive loads.

### 3. Select EMW Configurations

The several orientations of the EMWs spacecraft control system are possible. The requirements for integrating the momentum management and energy storage functions have been well established (Flatley, 1983). Figure 3-1 shows typical orientations of EMWs relative to satellite control axes. From these, the initial EMW configuration selected for the satellite system simulation presented in Section 7 utilized four EMWs oriented along the legs of a 4-sided pyramid and is identified as the Conical configuration. The simulation considered imperfect balancing of momentum and energy by incorporating the EMWs into attitude control law of the simulated spacecraft. Additionally, the shafts of the rotors need not assume a perfect alignment. Spacecraft typically achieve a 0.1 degrees of alignment of components. By allowing specification of misalignment (say .001



to .1 degrees), the simulation calculates momentum going to other axes and demonstrates the result of this “real-world” effect.

#### 4. A Proposed Algorithm Combining Energy Management and Momentum Control

The algorithm discussed below presents a method for storing and retrieving energy using a system of energy momentum wheels. A few of the attributes of using a Energy Momentum Wheel Assembly (EMWA) are replacing chemical batteries and momentum unloading devices (e.g. magnetic torquer bars) by combining two subsystems the Attitude Control System (ACS) and the Electrical Power Supply System (EPS) into one EMWA thus simplifying spacecraft designs. Because the ACS system requires a spatial body torque another degree of freedom is required so the power supply algorithm can be executed within the null space defined by the EMWA alignment. Consequently, a minimum of four EMW devices is required to control a spacecraft's attitude and store energy (Flatley, 1985, and Tsiotras, 2001). A four-wheel Conical Configuration is assumed in this discussion.

Simulations show that if kinetic energy is unevenly distributed among the wheels that gyroscopic torques will become significant. This is due to the large angular momentum required on each wheel. In order to increase performance, a min-max distribution law (which is used on the Tropical Rainfall Measurement Mission (TRMM) and the Hubble Space Telescope (HST)) can be implemented as a low frequency process during the charging period so that each wheel maintains approximately equal momentum magnitude. Furthermore, a buffer zone must be maintained such that the ACS can issue torques without saturating the wheels. An implementation of the min-max distribution law is presented in Section 5.

## Symbols

$\omega_i$  , angular velocity of the i-th wheel

$\tau_{iACS}$  , ACS control torque described in the EMWA frame issued to the i-th wheel

$\tau_{PS}$  , power supply control torque magnitude

$\tau_{iTOTAL}$  , the total torque issued to the i-th wheel

$P_{EMW}$ , power charging or discharging the EMWA

$P_{load}$ , power load required by system

$P_{S/A}$ , power supplied by solar arrays

$P_{ACS}$ , power generated by ACS control torques

$e_i$ , spin axis described in the s/c body axis of i-th wheel

## Algorithm

To keep matters clear and simple a Conical (pyramid) Configuration, shown in Figure 3-1, is specified as:

$$e_1 = (1.0, 0.0, 1.0) / \sqrt{2.0},$$

$$e_2 = (0.0, 1.0, 1.0) / \sqrt{2.0},$$

$$e_3 = (-1.0, 0.0, 1.0) / \sqrt{2.0}$$

$$e_4 = (0.0, -1.0, 1.0) / \sqrt{2.0}$$

The null vector is defined as  $n = (-1.0, 1.0, -1.0, 1.0)$ .

At any given time suppose the ACS has determined a control torque  $\tau_{ACS}$  is to be issued which is described in the EMWA frame. The power generated by this torque is

$$P_{ACS} = \tau_{1ACS} \omega_1 + \tau_{2ACS} \omega_2 + \tau_{3ACS} \omega_3 + \tau_{4ACS} \omega_4$$

In addition, the charging (or discharging) power at this same instant is  $P_{S/A} - P_{load}$  (Bartlett, et.al., 1997).

$P_{EMW}$  charges the wheels by compensating for the power loss due to the ACS control and is determined by

$$P_{EMW} = P_{S/A} - P_{load} - P_{ACS} = P_{S/A} - P_{load} - (\tau_{1ACS} \omega_1 + \tau_{2ACS} \omega_2 + \tau_{3ACS} \omega_3 + \tau_{4ACS} \omega_4).$$

Since

$$P_{EMW} = \tau_{PS} n \cdot \omega, \text{ where } \omega \text{ is the } 4 \times 1 \text{ wheel angular velocity vector}$$



$$P_{EMW} = -\tau_{PS} \omega_1 + \tau_{PS} \omega_2 - \tau_{PS} \omega_3 + \tau_{PS} \omega_4 = P_{S/A} - P_{load} - (\tau_{1ACS} \omega_1 + \tau_{2ACS} \omega_2 + \tau_{3ACS} \omega_3 + \tau_{4ACS} \omega_4)$$

This implies

$$\tau_{PS} = [P_{S/A} - P_{load} - (\tau_{1ACS} \omega_1 + \tau_{2ACS} \omega_2 + \tau_{3ACS} \omega_3 + \tau_{4ACS} \omega_4)] / (-\omega_1 + \omega_2 - \omega_3 + \omega_4)$$

As a result the modified torque commands issued to the wheels are

$$\tau_{1TOTAL} = \tau_{1ACS} - \tau_{PS}$$

$$\tau_{2TOTAL} = \tau_{2ACS} + \tau_{PS}$$

$$\tau_{3TOTAL} = \tau_{3ACS} - \tau_{PS}$$

$$\tau_{4TOTAL} = \tau_{4ACS} + \tau_{PS}$$

## 5. Momentum Distribution Law

The following discussion is based on work performed at GSFC on such satellites as the Tropical Rainfall Mapping Mission (TRMM) (Bromberg, 19XX). The EMWs will use this momentum distribution law in order to minimize the wheel speeds and prevent the EMWs from spinning up to high rates that would saturate the wheels and thus render the control useless. Four unit vectors (e1, e2, e3, e4) define the orientation of the EMWs. The components of these vectors are defined by the direction cosines in the spacecraft coordinate frame. The polarity is defined positive if a positive voltage applied to the EMW results in a wheel torque that will spin the EMW in a counterclockwise direction consistent with the right hand rule.

Wheel Orientation Matrix (3x4):

$$[M] = [e1, e2, e3, e4]$$

Steering Matrix (PseudoInverse 4x3):

$$[SM] = M' * INVERSE(M * M')$$

PID control Torque Vector (3x1):

$$TC = [TX, TY, TZ]' \text{ i.e. roll, pitch, yaw}$$

Wheel Control Torque (4x1):

$$TCMDemw = [SM] * TC$$

Wheel Vector Torque (3x1):

$$TC = [M] * TCMDemw = [M] * [SM] * TC$$

The EMW wheel vector torque that applies the reaction control to the spacecraft is equal to the control torque defined from the PID controller. The 4 unit vectors must be linearly dependent in the spacecraft coordinate frame. Since any 4 vectors must be linearly dependent in a 3-dimensional vector space, there exists a nonzero linear combination that sums to zero. Let {A1, A2, A3, A4} be a set of normalized coefficients which satisfy the dependent vector equation,

$$A1 * e1 + A2 * e2 + A3 * e3 + A4 * e4 = 0 \text{ ( where at least one of the } A_i \text{ is not zero)}$$

For a Conical (or pyramid) Configuration, all the coefficients will satisfy the absolute condition

$$|A1| = |A2| = |A3| = |A4| = 1$$

If "f" is any scalar function, the equality is maintained by multiplication by scalar "f",

$$f*(A1*e1 + A2*e2 + A3*e3 + A4*e4) = 0$$

Let Hemw = set of wheel momentum defined by the product of wheel inertia and wheel speed (rad/sec),

$$\{Hemw\} = \{HEMW1, HEMW2, HEMW3, HEMW4\} \text{ N-m-sec}$$

The system wheel momentum is than the vector sum of each of the wheels

$$hw = HEMW1*e1 + HEMW2*e2 + HEMW3*e3 + HEMW4*e4$$

An equivalent set of wheel momenta having the same system wheel momenta but different wheel speeds is obtained by adding the "null vector".

$$hw = (HEMW1+f*A1)*e1 + (HEMW2+f*A2)*e2 + (HEMW3+f*A3)*e3 + (HEMW4+f*A4)*e4$$

Since none of the Ai's = 0, the equivalent form is:

$$hw = (HEMW1/A1+f)*A1*e1 + (HEMW2/A2+f)*A2*e2 + (HEMW3/A3+f)*A3*e3 + (HEMW4/A4+f)*A4*e4$$

Driving each of the wheels to its lowest equivalent wheel momentum minimizes the absolute wheel speeds.

$$Heqrw = \{ HEMW1/A1+f, HEMW2/A2+f, HEMW3/A3+f, HEMW4/A4+f \} \text{ N-m-sec}$$

$$\text{Let } Hmax = \max\{HEMW1/A1, HEMW2/A2, HEMW3/A3, HEMW4/A4\} \text{ N-m-sec}$$

$$\text{Let } Hmin = \min\{HEMW1/A1, HEMW2/A2, HEMW3/A3, HEMW4/A4\} \text{ N-m-sec}$$

Then  $|Heqrw|$  is minimized when  $(Hmin + f) = -(Hmax + f)$ . Hence,  $f = -(Hmax + Hmin) / 2$ . Note that when  $Hmin = -Hmax$ , it implies that  $f=0$  which is a necessary condition to be at the optimum wheel speed. If the distribution law is to drive the wheels to its minimum wheel speed without producing a disturbance torque to the spacecraft, a control torque proportional to "f" should be applied to each wheel. A simple control law uses a constant proportional gain "K" as

$$Tdist = K*f$$

$$Tdist = -0.5*K*(Hmax + Hmin)$$

Next, minimizing the absolute wheel speeds relative to a bias momentum, Hbias modifies the above approach,

$$-H_{bias}*(A1*e1 + A2*e2 + A3*e3 + A4*e4) = 0$$

Hence,

$$H_w = (HEMW1 + (f - H_{bias}) * A1) * e1 + (HEMW2 + (f - H_{bias}) * A2) * e2 + (HEMW3 + (f - H_{bias}) * A3) * e3 + (HEMW4 + (f - H_{bias}) * A4) * e4$$

which results in  $(f - H_{bias}) = - (H_{max} + H_{min})/2$  such that  $f = H_{bias} - (H_{max} + H_{min})/2$ . Again note that when  $(H_{min} - H_{bias}) = -(H_{max} - H_{bias})$ , that it implies  $f=0$  which is a necessary condition to be at the optimum wheel speed.

$$T_{dist} = K * f$$

$$T_{dist} = -0.5 * K * (H_{max} + H_{min} - 2 * H_{bias})$$

where

Wheel Orientation Constraint Vector (4x1):  $AI = \{A1, A2, A3, A4\}'$  where

$$[M] * AI = 0$$

Modified Distribution Torque Command (4x1):  $T_{cmd} = T_{CMDemw} -$

$$T_{dist} * AI$$

Modified Wheel Vector Torque (3x1)

$$TC = [M] * T_{cmd}$$

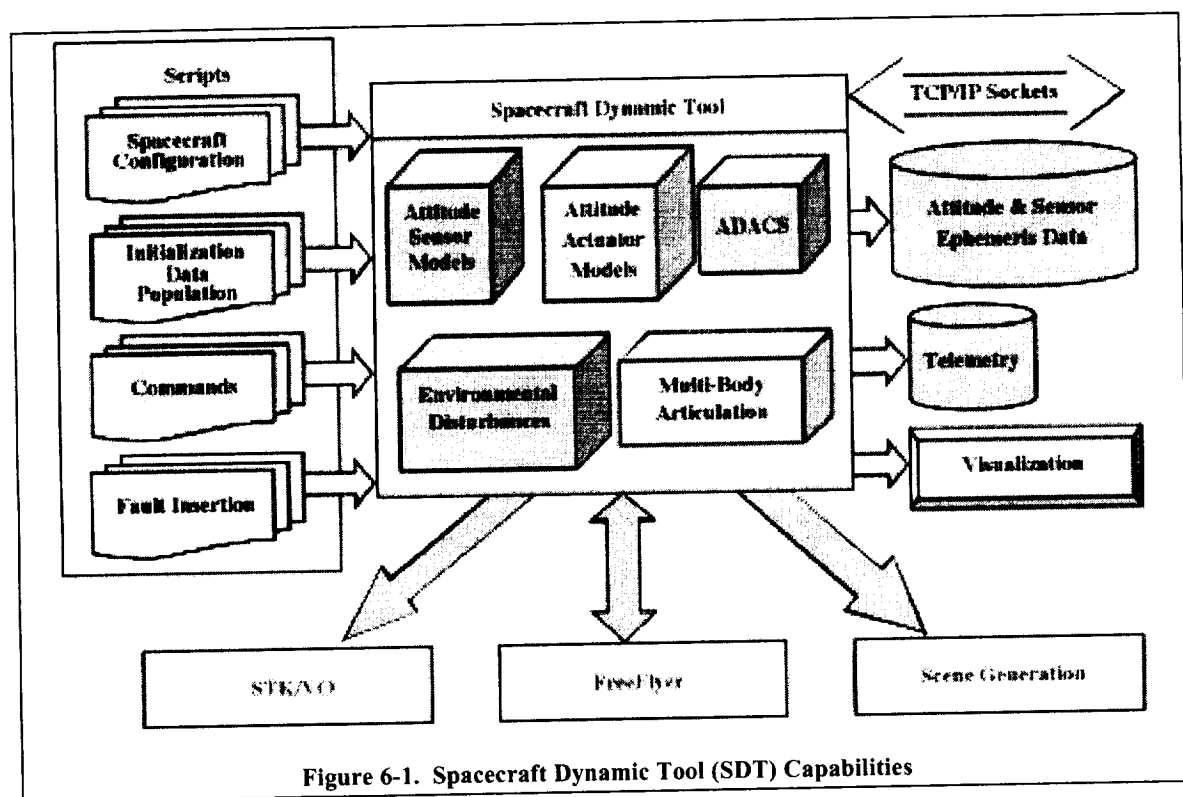
The modified wheel vector torque that applies the reaction control to the spacecraft is equal to the control defined from the PID controller. The distribution torque applies no net torque to the spacecraft and applies no net torque to the wheels. since no net torque is applied to the distribution torque can not change the spacecraft dynamics or system wheel momentum. The system stability is therefore governed by the stability of the PID controller. Since the vector sum of wheel momentum is not changed, the distribution law is transparent to the magnetic unloading system and therefore may act independently. To prevent the wheel speeds from going into deep saturation, which would render a loss of the PID control torque, the distribution torque is applied to redistribute the wheel momentum vector amongst the four wheels to run the wheels at the minimum wheel speed.

## 6. Simulation of a Spacecraft Using EMWs

In order to demonstrate the suitability and benefit of integrating EMWs into a spacecraft, a satellite system simulation was developed to establish controls requirements and verify performance. Additionally, the simulation provides system guidance for the development of the EMW. The EMW Spacecraft System Simulation incorporates the measurement of key parameters and the modeling of the system elements of a modern spacecraft including an inertial reference systems, coarse sun sensors, fine sun sensors, three axis

magnetometers, earth sensors, actuator models (multiple EMWs, magnetic torque coils/bars, and thrusters). The simulation includes virtually all of the relevant space environment and orbital parameters of interest including gravitational models of the sun and moon, solar wind, near earth magnetic fields, atmospheric density, gravity gradients, sensor/actuator noise disturbances, and internal system disturbances such as rotating antennas and solar arrays. This simulation has provision for incorporating new modules, such as star trackers, to expand its capabilities. A systems approach is fundamental to incorporating an EMW into a satellite. As a component of both the attitude control subsystem and the power subsystem, the EMW requires a multi-discipline vision of the spacecraft designer.

The original WinSIM32 simulation has been converted to Microsoft Foundation Class(MFC) C++ where the coding is directed to being a truly object oriented simulation. This simulation, shown in Figure 6-1, is called Spacecraft Dynamic Tool, (SDT) (Strunce, 1999). The EMW Spacecraft System Simulation was implemented using SDT.



Sun, Moon, and Earth Classes have been created where the Earth Class includes the Atmosphere, Gravity and Magnetic field. Each sensor and actuator type has been converted to a Class of Assembly Types. That is, the user can create a sensor block such

as a Coarse Sun Sensor(CSS) with 'n' number of CSS sensors within that CSS Assembly Block as graphically indicated in Figure 6-2 below.

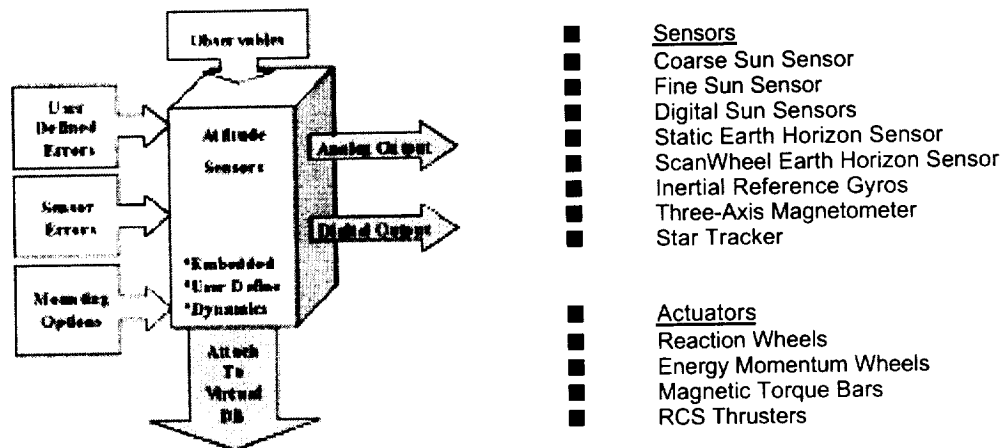


Figure 6-2. Sensor & Actuator Assemblies

All the data for those sensors are encapsulated within the Class as well as the models and algorithms. The initiation of that sensor block automatically attaches the data to a Virtual Data Base (VDB). The User has access to the VDB to edit or modify data. A 'State Vector' Class was created to integrate the system dynamic states. The 'State Vector' automatically looks for the Assembly Types or Objects, requests the derivatives from the dynamic models, integrates the derivatives and returns the states back to the respective Assembly Objects. This is transparent to the User.

During this effort, the EMW model, the power system model and the EMW controls algorithms were developed, integrated and verified with the SDT. Initial simulations of the integrated simulation have been performed. Initially, a single EMW was demonstrated to interact with the power system. The EMW was integrated with the reaction wheel model to incorporate the spacecraft control interface. This new object was then integrated as four separate units and a null momentum algorithm was implemented to maintain a constant momentum vector while the EMWs were charged and discharged over several orbits.

## 7. Simulation of Simultaneous Energy Storage and Attitude Control

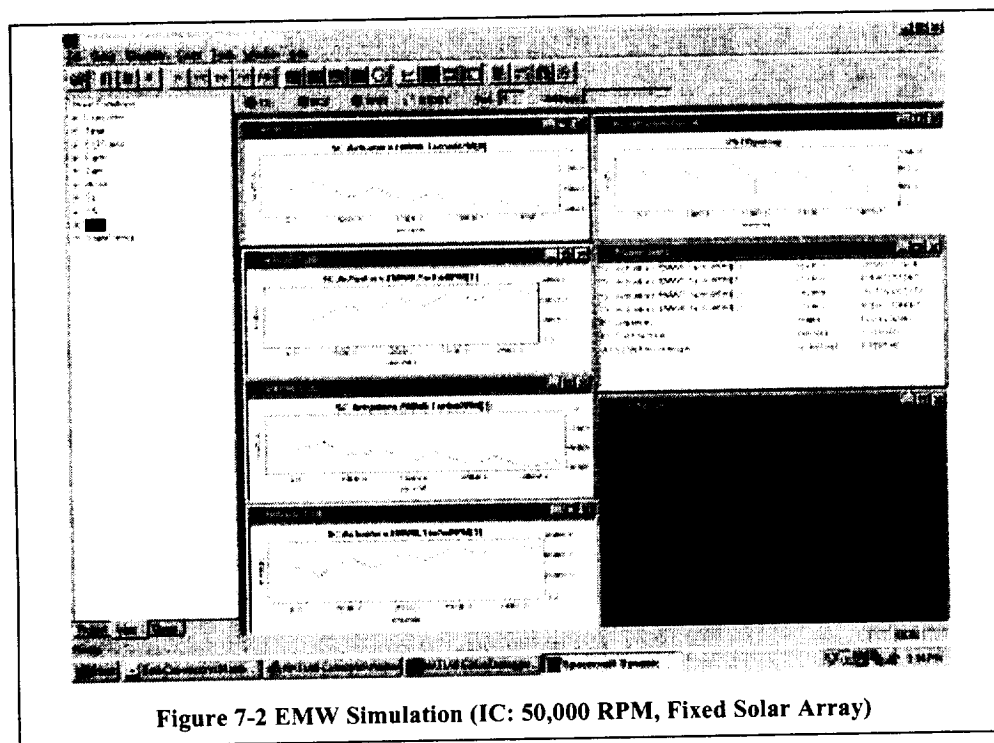
To assess the accuracy and utility of the EMW Spacecraft System Simulation, a straw man nadir oriented MIDEX class mission was synthesized. A 1200 watt nominal output solar array was selected to support a 450 watt continuous power to the spacecraft. A

nominal 600 km altitude orbit was selected. Both high (53°) and low (equatorial) inclinations were studied. The principal moments of inertia (MOI) were 1000, 500, 700 kg m<sup>2</sup> about the roll, pitch, and yaw (x,y,z) respectively. A four EMW configuration of the conical (or square pyramid) type, as described earlier in Section 4.3.1, was selected. The characteristics of the EMW are presented in Table 7-1.

**Table 7-1 Selected Characteristics of the Simulated EMW**

EMW MOI	0.02961 kg m <sup>2</sup>	Momentum Limit:	280 N m sec
Maximum EMW Speed:	90,000 RPM	Max Power per EMW:	800 watts
Maximum Energy Storage:	365 w hr (in each of 4)	Initial EMW Speed:	50,000 RPM

The first simulation result is presented in Figure 7-2. This simulation ran for about



28,000 seconds of orbital time in just under 3000 seconds, or about 10 times real time. The figure presents time (strip chart) plots of the four EMW wheel speeds and the power supplied by the solar array. A numerical window displays several spacecraft parameters (valid at simulation time) and a graphic of the orbit and its spherical ground trace. On the left side of this figure is the hierarchical virtual data base tree, described earlier. For this

simulation, the solar array was assumed to be rigidly mounted to the spacecraft and facing outward in an anti-nadir direction. At the start of the simulation, the EMW has an angular velocity of 50,000 RPM. Given the assumed maximum speed of 90,000 RPM, EMW was 70% discharged. Because the solar array did not track the Sun, the initial output of the edge-on array is low, even though it would be cold and more efficient. The resulting energy produced by the solar array in approximately five orbits was sufficient to fully recharge the EMWs and provide the specified bus power.

In the second simulation, the initial conditions of the EMWs and the characteristics of the

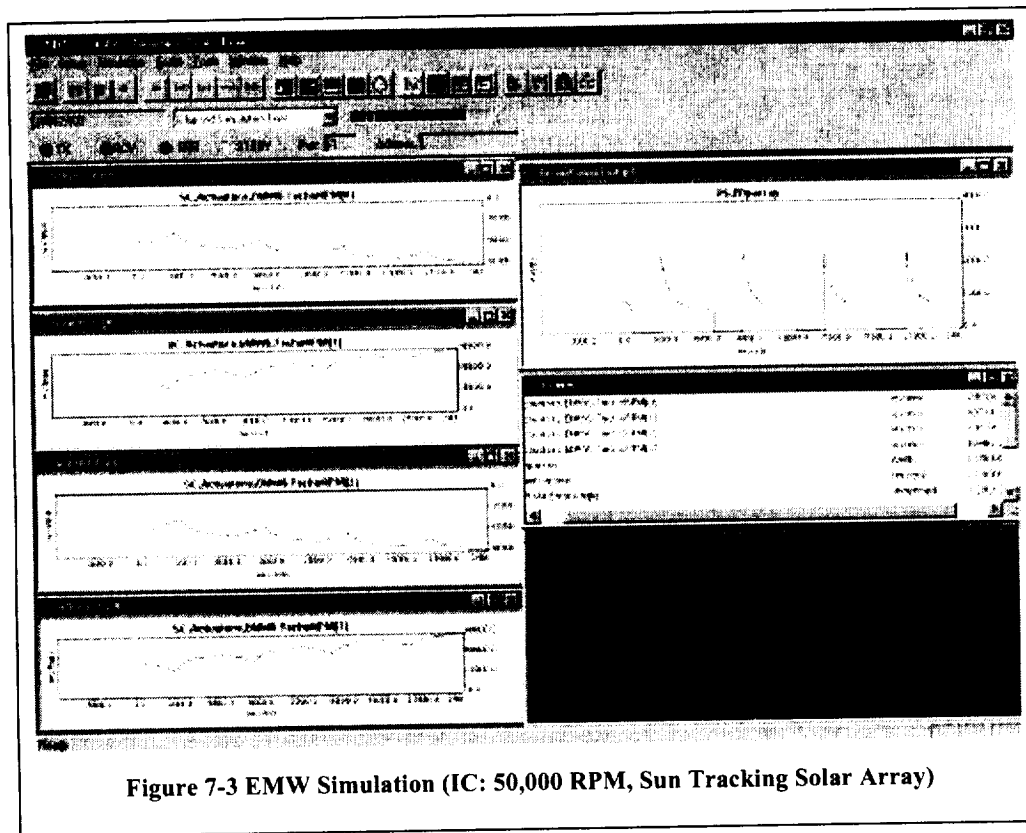
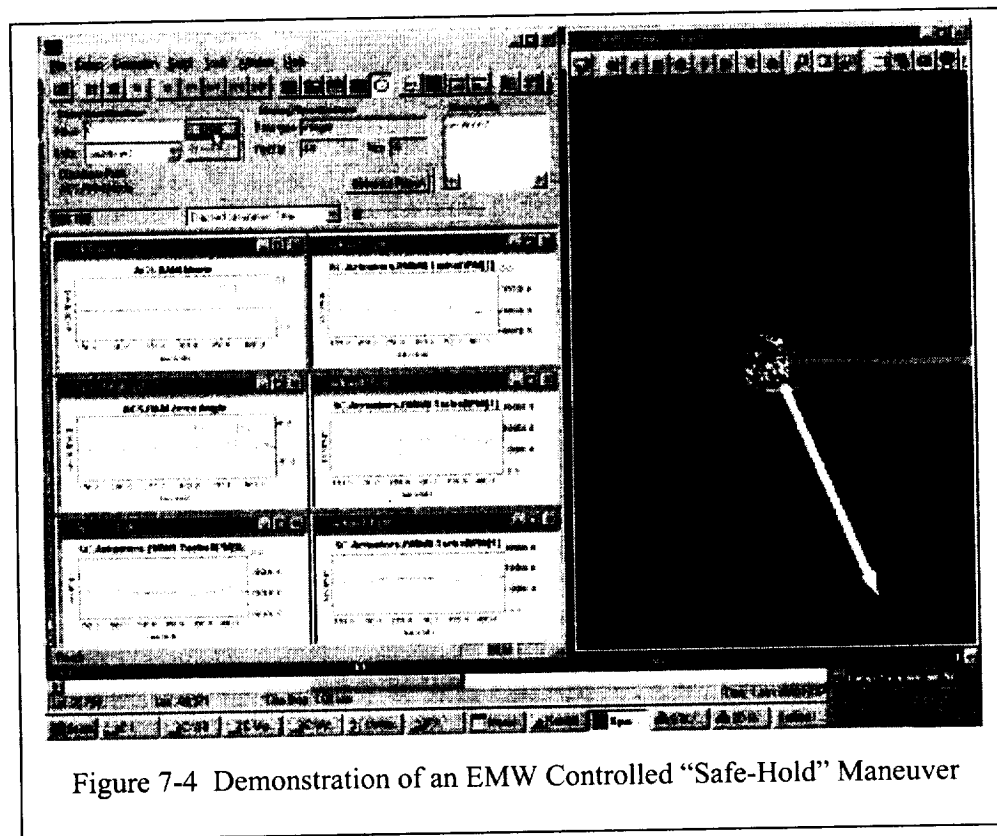


Figure 7-3 EMW Simulation (IC: 50,000 RPM, Sun Tracking Solar Array)

spacecraft were the same except the array was commanded to track the sun line. Figure 7-3 presents the simulation result. The EMW is a maximum power point tracking device and is able to benefit from the higher than rated power output of a cold solar array. With the benefit of a sun-tracking array, the EMWs are fully recharged in about four orbits, a full orbit sooner than without a tracking array.

The ability of the EMWs to slew a spacecraft is simulated in Figure 7-4. The simulation begins in a nadir pointing orientation. The spacecraft is then commanded to point to the Sun (Safe-Hold Mode). At about 300 seconds after the start of the simulation, the ACS RAM Mode is commanded to a "1" state. This command caused the orientation of the

spacecraft to move to align its yaw axis with the sun line, like a typical Safe Hold maneuver. In the simulation's Attitude Control Subsystem (ACS), a parameter identified as the ACS RAM Error Angle is developed that indicates the combined pointing error about roll, pitch, and yaw as an absolute number. Following the Safe Hold command, the ACS RAM Error Angle rises and the spacecraft begins to move toward the sun line. The EMWs exchange energy between them and impart momentum to the spacecraft. At about 375 seconds, the spacecraft-pointing angle is approaching the sun line and the spacecraft rates are reduced as the EMWs tend toward their pre-maneuver distribution of energy.

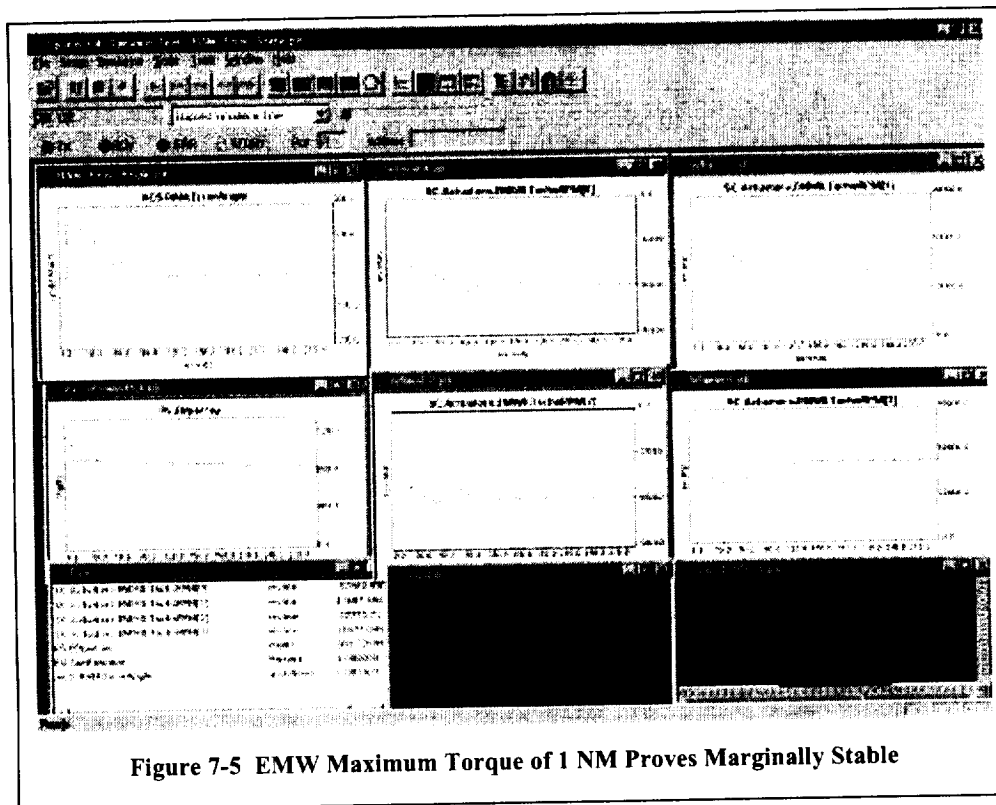


At that time the spacecraft is commanded back to nadir pointing, and the maneuver is reversed as the EMWs exchange energy in the opposite sign from the first maneuver. The simulation is stopped as the spacecraft is returning to nadir pointing and the EMWs are returning to their pre-maneuver energy levels (RPMs). The three-dimensional spacecraft image on the right is demonstrating the linkage of the EMW Spacecraft Simulation (using SDT) to the Visualization Option of the Satellite Tool Kit (trademark, Analytical Graphics). The image follows the attitude and orbit position commands from the EMW Spacecraft Simulator to aid understanding the affects of EMW rotor speed on the spacecraft's attitude.



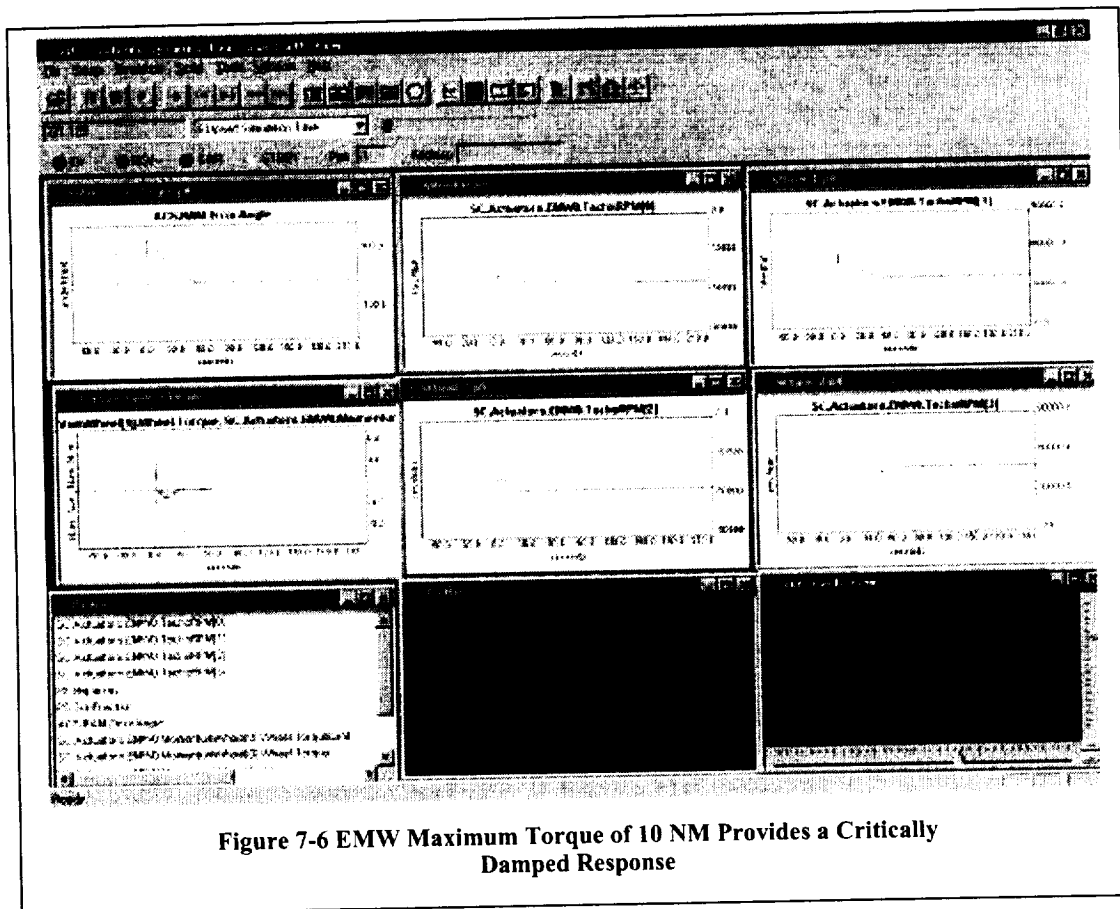
The next series of simulations demonstrates the ability of the EMW Spacecraft Simulation to aid in the development of performance specifications for the EMW. The EMWs are initially allowed to produce a maximum of 1 NM of torque. The initial condition of the spacecraft is off-pointed from the desired attitude by 30°, 60°, 90° (x,y,z) with body rates of 1°, 2°, 3°/second (x,y,z). As the simulation starts the EMWs exchange energy to damp the body rates and drives the spacecraft to the desired orientation. Capturing of the spacecraft proceeds smoothly for the first 45 seconds and then the pointing error starts to increase up until about 75 seconds when the EMWs recover the spacecraft and achieve a critically damped pointing maneuver.

The maximum allowed EMW torque is then increased to 10 NM. The simulation presented in Figure 7-6 demonstrates a smooth critically damped capture of the desired spacecraft attitude from the same initial condition of the simulation shown in Figure 7-5.



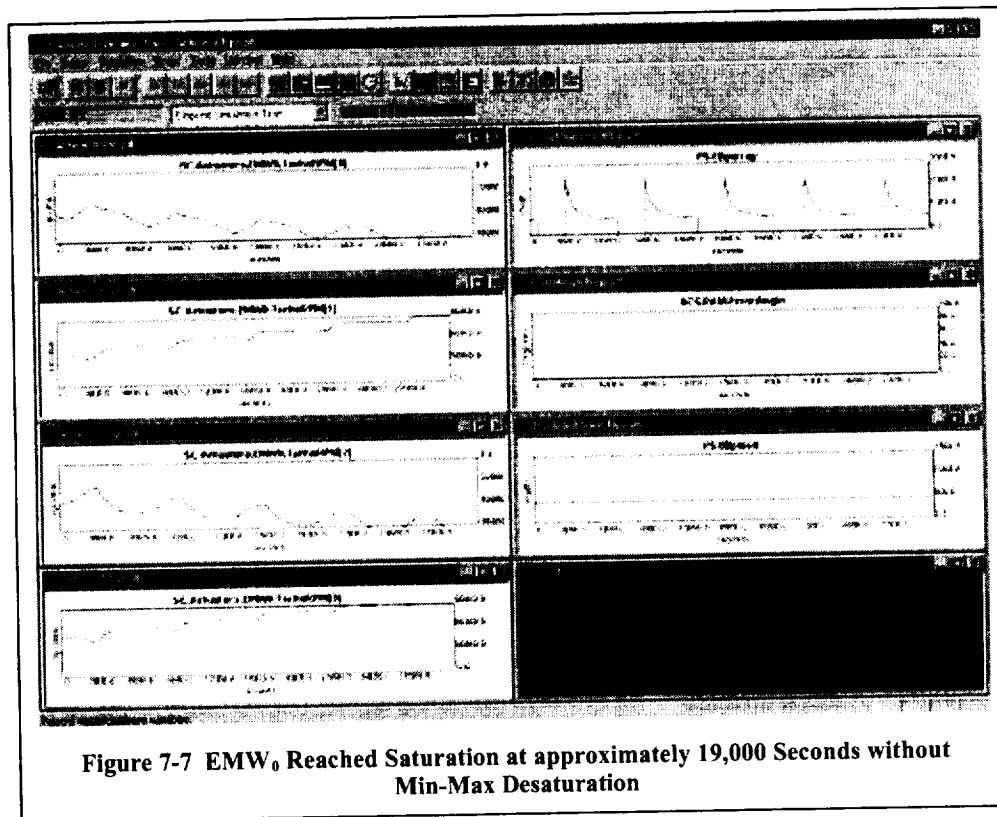
The last sequence of simulations demonstrates the effect of the EMWs starting the simulation at different levels of energy. EMW<sub>0</sub> was assigned an initial angular velocity of 60,000 RPMs. EMW<sub>1</sub> was assigned a speed of 40,000 RPMs. EMW<sub>2</sub> and EMW<sub>3</sub> were each started at 50,000 RPMs, as was done in all of the previous simulations. A momentum imbalance between the EMWs could rise from initial conditions or from the cancellation of secular torques over a period of time. The concern being addressed is that

no EMW should be allowed to reach its maximum speed and saturate. The EMW must



be able to create both positive and negative torques by accepting or supplying energy in order to maintain a neutral momentum vector. Therefore, a buffer zone below the maximum speed needs to be maintained. As shown in Figure 7-7, EMW<sub>0</sub> reached saturation after about 19,000 seconds of the simulation when no control law was used to desaturate the EMWs. At that point it would not have been able to increase its speed and it would have been lost to the remaining EMWs as a potential energy source/sink.

The simulation in Figure 7-8 had identical initial conditions to that presented in Figure 7-7, but the TRMM momentum distribution law discussed in Section 5 was active. In the latter case, a momentum margin of about 20% below maximum speed was maintained, even though the EMWs were not operating with equal levels of energy in each EMW. The ability of the EMW Spacecraft Simulation to demonstrate such a system consideration early in the EMW design process will assure the incorporation of necessary margin in EMW specifications. The use of analytical tools, such as the EMW Spacecraft Simulation, to guide the EMW design processes supports the goals of concurrent engineering.



## 8. Conclusion

In this paper, we have discussed the motivation to utilize Energy Momentum Wheels (EMWs) to combine spacecraft attitude control and energy storage, and a few alternative configurations were presented. Critical elements of an EMW were discussed and a spacecraft system simulation utilizing a conical EMW configuration was used to demonstrate the concept of combined energy storage and attitude control for a MEDEX class spacecraft. A combined energy storage and attitude control law was presented and tested for a limited set of initial conditions. The simulation and initial conditions were configured using a script language. This flexibility allows the simulation tool to be used to evaluate a wide range of spacecraft missions and configurations incorporating EMWs.

A NASA Glenn sponsored laboratory demonstration of combined energy storage and two-axis spacecraft attitude control is currently under development at Lockheed Martin CSS Newtown, with results expected in about two years. Hardware development of a high specific energy EMW prototype has begun with private funding. The completion of this latter development is expected in a two to three year timeframe. Once demonstrated, the EMW could change the architecture of many future spacecraft.

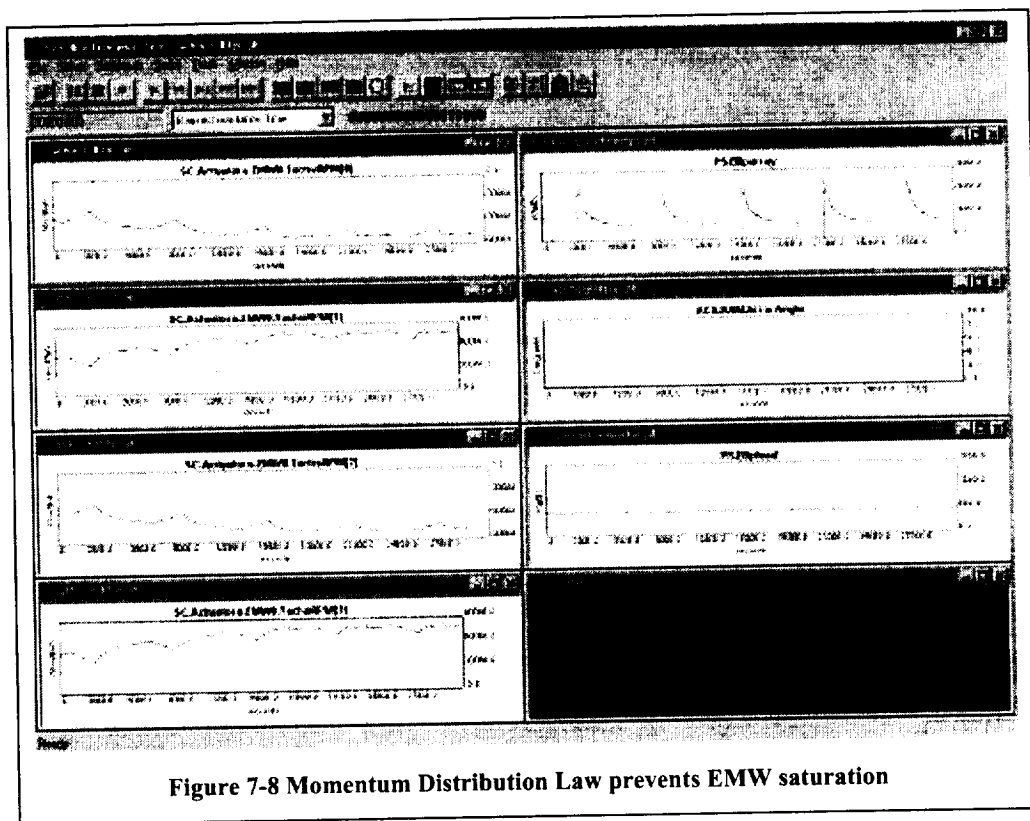


Figure 7-8 Momentum Distribution Law prevents EMW saturation

## References:

Bartlett, R., et.al., Energy Momentum Wheels for Satellites and Other Applications with Gain Scheduled Controllers, SBIR Phase I Final Report, Contract NAS 5-97073, September, 1997.

Bromburg, B., (ADD TRIMM MOMENTUM MANAGEMENT REFERENCE)

Flatley, Thomas W., and Hoffman, Henry C., "*Attitude Control and Energy Storage Flywheels*," Integrated Flywheel Technology 1983: Proceedings of a workshop held at NASA Goddard Space Flight Center, Greenbelt, Maryland, NAS 1.55:2290, August 2-3, 1983.

Flatley, T., "Tetrahedron Array of Reaction Wheels for Attitude Control and Energy Storage," Proceedings of the 20th Intersociety Energy Conversion Engineering Conference, Vol. 2, 1985, pp. 2353-2360.

Luo, J., et.al., "Implementation Results of  $\mu$ -Synthesis Control for an Energy Storage Flywheel Test Rig, 7th International Symposium on Magnetic Bearings, Zürich, Switzerland, August 2000.

Strunce, R., and Maher, F., "An Object Oriented Simulation Architecture For Rapid Spacecraft Prototyping," Flight Mechanics Symposium, NASA, Goddard Space Flight Center, Greenbelt, MD, May 18-20, 1999.

Tsiotras, P., et. al., "Satellite Attitude Control and Power Tracking with Momentum Wheels" AAS/AIAA Astrodynamics Specialist Conference, Girdwood, Alaska 16-19 August 1999.

Tsiotras, P., et.al. "Satellite attitude Control and Power Tracking with Energy/Momentum Wheels", Journal of Guidance, Control, and Dynamics, Vol. 24, No. 1, January-February 2001, pp. 23-34.

Zorzi, E.S., et.al, "Stabilization of a High Speed Rotor with Active Magnetic Bearings by a Piecewise  $\mu$ -Synthesis Controller." 6th International Symposium on Magnetic Suspension Technology, Torino, Italy, October, 2001.